Donor dendritic cell-derived exosomes promote allograft-targeting immune response

Quan Liu, Darling M. Rojas-Canales, Sherrie J. Divito, William J. Shufesky, Donna Beer Stolz, Geza Erdos, Mara L.G. Sullivan, Gregory A. Gibson, Simon C. Watkins, Adriana T. Larregina, and Adrian E. Morelli.

Supplemental data includes:

Supplemental figures 1-12

Supplemental video legends

Supplemental methods

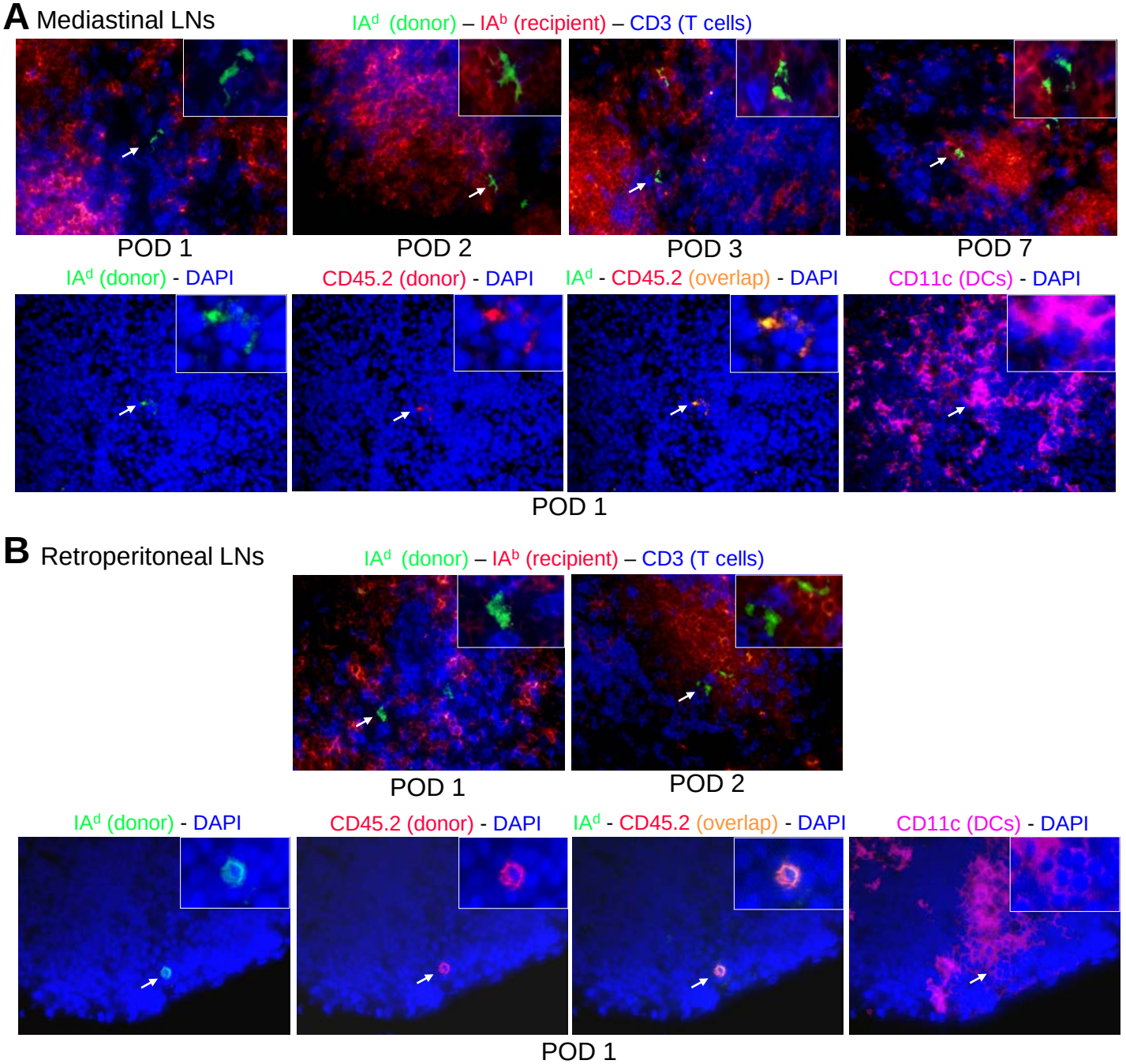

Figure S1 legend (next page).

Figure S1. Detection of donor DCs in graft-draining lymph nodes after fully mismatch heterotopic (abdomen) cardiac transplantation in mice. (**A**) Upper panel, detection by immuno-fluorescence microscopy of donor (BALB/c) migrating cells (IA^{d+} $CD45.2^{+}$) in T-cell areas ($CD3^{+}$) of mediastinal lymph nodes (LNs) of recipient (B6, $H2^{b}$ $CD45.1^{+}$) mice, on successive PODs. Bottom panel, the identity of the migrating BALB/c cells as DCs was confirmed by co-expression of the DC-marker CD11c in combination with CD45.2 and IA^{d} (both from BALB/c). The cells indicated by arrows are shown in the insets. Immuno-fluorescence microscopy. X 200. Representative images of mediastinal and retroperitoneal lymph nodes are shown, out of 3 mice per POD. (**B**) Mobilization of donor (BALB/c) cells (IA^{d+} $CD45.2^{+}$) to T-cell areas ($CD3^{+}$) of retroperitoneal lymph nodes of recipient (B6, $H2^{b}$ $CD45.1^{+}$) mice analyzed as in (**A**). Donor IA^{d+} cells were undetectable by microscopy in retroperitoneal lymph nodes on PODs 3 and 7 (not shown). (**C**) Donor (BALB/c) cells mobilized to mediastinal and retroperitoneal lymph nodes of the recipients were undetectable by quantitative genomic real time PCR designed for detection of the H2-Eα gene (encoded in BALB/c DNA, absent in B6), and with a detection limit of up to 1 BALB/c cell in 10^{6} B6 cells. Representative samples of mediastinal and retroperitoneal lymph nodes per POD are shown (out of 3 samples per POD, run in triplicates). The straight light blue line indicates the PCR detection threshold.

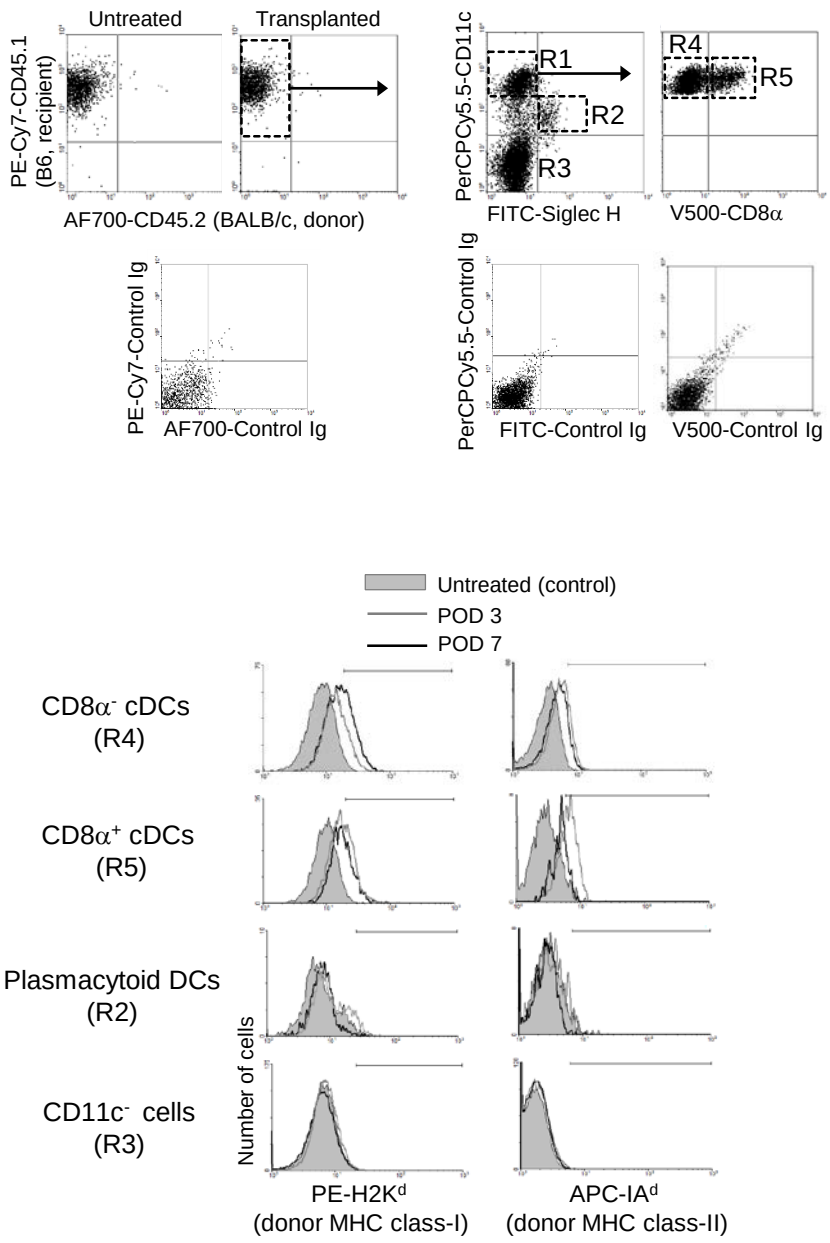

Figure S2. Strategy for detection of subpopulations of recipient (B6) splenic APCs by flow cytometry. (**A**) Recipient splenocytes were gated out of donor cells, or clusters of donor plus recipient leukocytes, by their CD45.1 expression and lack of CD45.2 labeling. Within the CD45.1^{+} CD45.2^{neg} recipient cell gate, cDCs and plasmacytoid DCs (pDCs) were identified by their CD11c^{high} Singlec H^{neg} (R1) and CD11c^{int} Singlec H^{+} (R2) phenotypes, respectively. Subsets of recipient cDCs were further analyzed based on their CD8α expression (R4 & R5). (**B**) Histograms showing subsets of recipient (B6) splenic APCs, based on the gating strategy depicted in (A), carrying on the cell surface donor-derived H2K^{d} and IA^{d} molecules, detected by FACS, on POD 3 and 7 after transplantation of BALB/c hearts, and in control (untreated) B6 mice. Representative histograms out of 3 mice per time point are shown.

5 nm $H2D^d$-IA^d

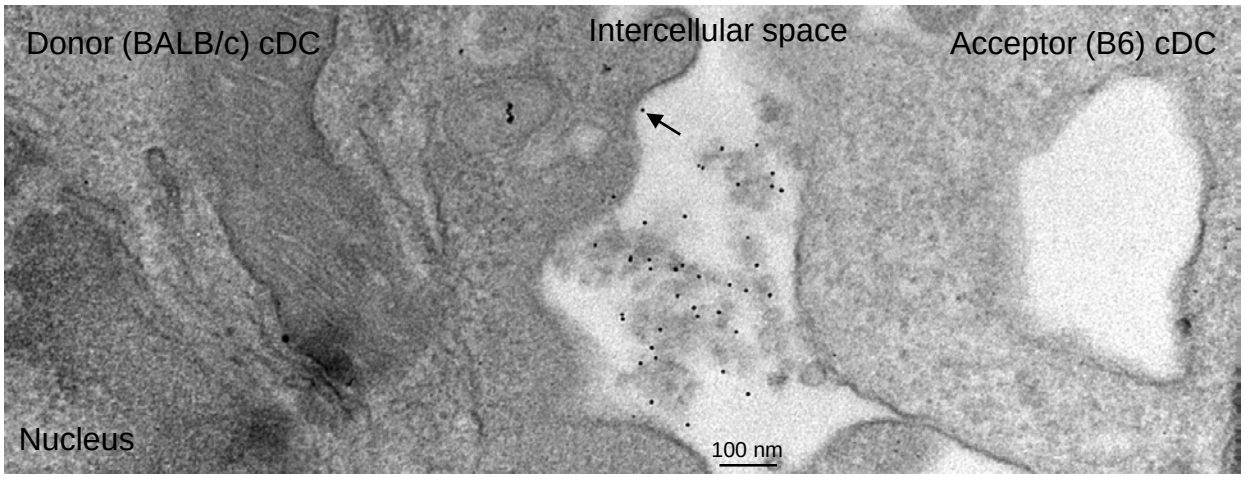

Figure S3. Transfer of EVs between donor and recipient cDCs. Transmission EM image of the intercellular gap between a donor (BALB/c) and an acceptor (B6) splenic cDC after 20 hour co-culture. The image shows the passage of a cluster of small EVs expressing $H2D^d$ and IA^d (from the BALB/c) to the recipient (B6) cDC. The donor (BALB/c) cDC is identified by the expression of BALB/c MHC directly on the cell surface (arrow). X 40,000.

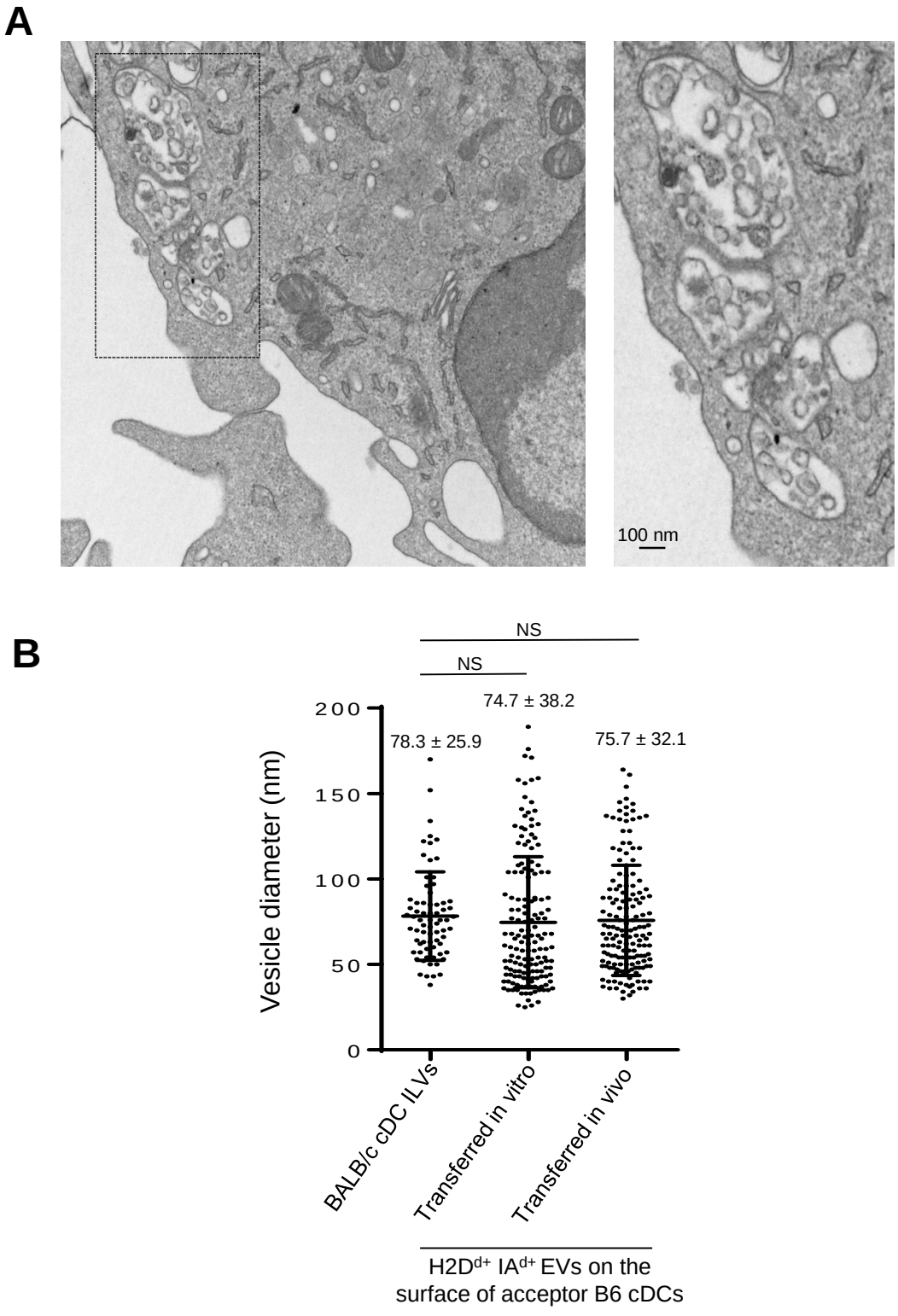

Figure S4. Size comparison between intraluminal vesicles (ILVs) in MVBs of cDCs and EVs transferred between cDCs. (A) Transmission EM image of MVBs with its cargo of ILVs in a BALB/c splenic cDC. The area in the rectangle is shown at higher magnification on the right. X 20,000-80,000. **(B)** Size comparison between ILVs in MVBs of BALB/c splenic cDCs, and BALB/c-derived ($H2D^{d+}$ IA^{d+}) EVs transferred to acceptor (B6) splenic cDCs. The vesicles were measured on EM images with the MetaMorph Offline 7.7.50 software. Results were analyzed by 1-way ANOVA, followed by Tukey-Kramer multiple comparisons test.

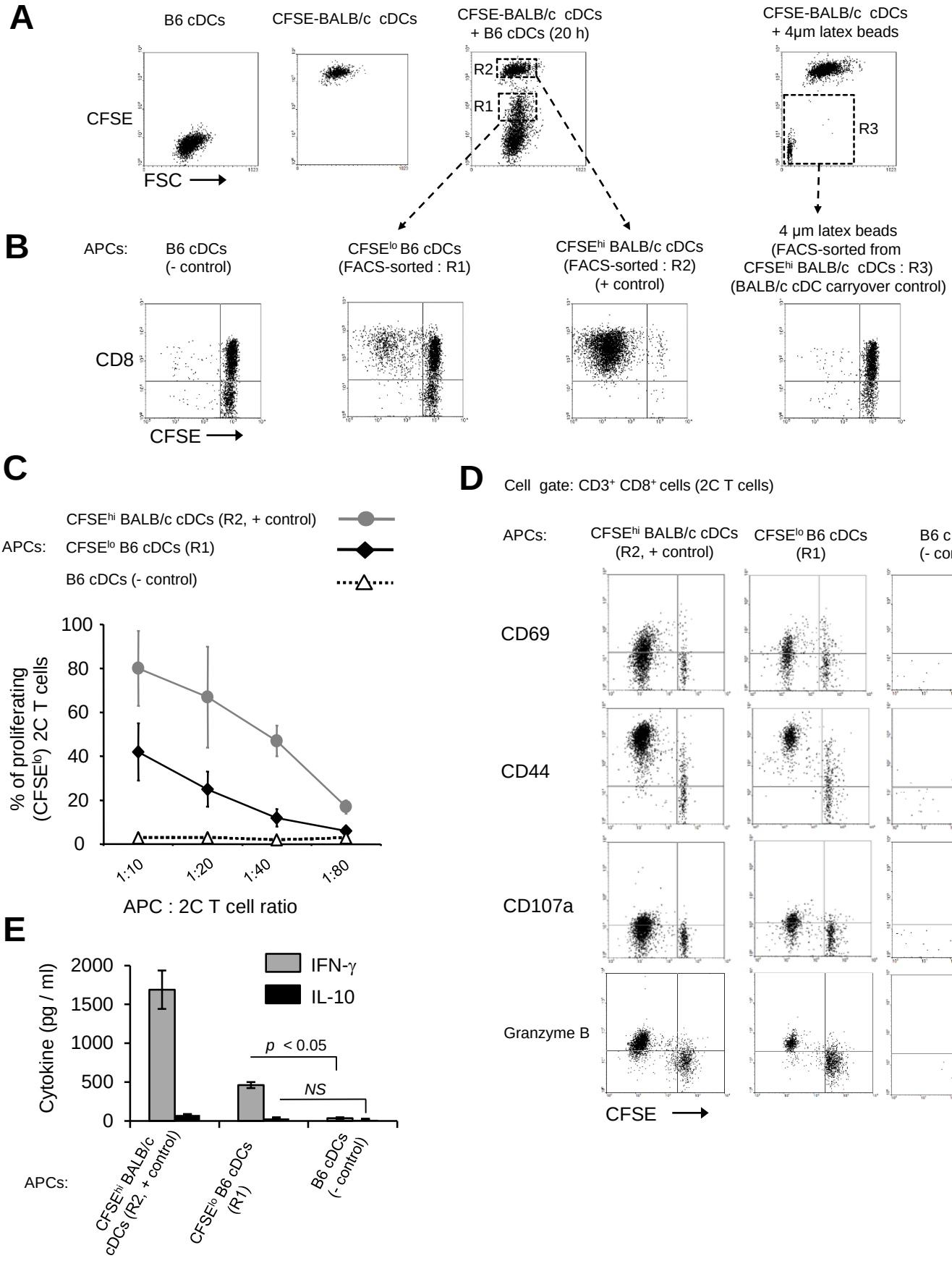

Figure S5 legend (next page).

Figure S5. B6 cDCs co-cultured with BALB/c cDCs promote proliferation and effector T cell differentiation of CD8 T cells against BALB/c MHC class I molecules. (**A**) FACS-sorting strategy for isolation of acceptor B6 splenic cDCs with $CFSE^{lo}$ content (R1, carrying the transferred MHC molecules), and $CFSE^{hi}$ donor (BALB/c) cDCs (R2) after 20 hour co-cultures. Latex beads (4 µm) cultured with $CFSE^{hi}$ BALB/c cDCs were sorted (R3) and used as negative controls in functional assays. (**B**) FACS-analysis of 3-day CFSE-MLCs showing that FACS-sorted $CFSE^{lo}$ B6 DCs triggered proliferation (by CFSE-dilution) of 2C CD8 T cells recognizing the BALB/c intact $H2L^d$ molecule. Latex beads FACS-sorted from co-cultures with $CFSE^{hi}$ BALB/c cDCs were used as carryover controls to demonstrate that presentation of $H2L^d$ molecules by B6 cDCs with $CFSE^{lo}$ content (R1) was not due to the presence of contaminating $CFSE^{hi}$ BALB/c cDCs. (**C-E**) Assessment of proliferation (by 3-day CFSE-MLCs) (**C**), expression of activation (CD44) and effector (CD107 and granzyme B) T-cell markers (by FACS) (**D**), and secretion of cytokines into MLC supernatants (by ELISA) (**E**), of CFSE-labeled 2C T cells stimulated with control cDCs or acceptor $CFSE^{lo}$ B6 cDCs FACS-sorted (R1 in **A**) from 20 hour co-cultures of B6 cDCs with $CFSE^{hi}$ BALB/c cDCs. IL-5 and IL-17A in MLC supernatants were below the limit of detection of the ELISAs. *P* values were generated by 1-way ANOVA followed by Tukey-Kramer multiple comparisons test. (**A-E**), one representative of 4 independent experiments is shown.

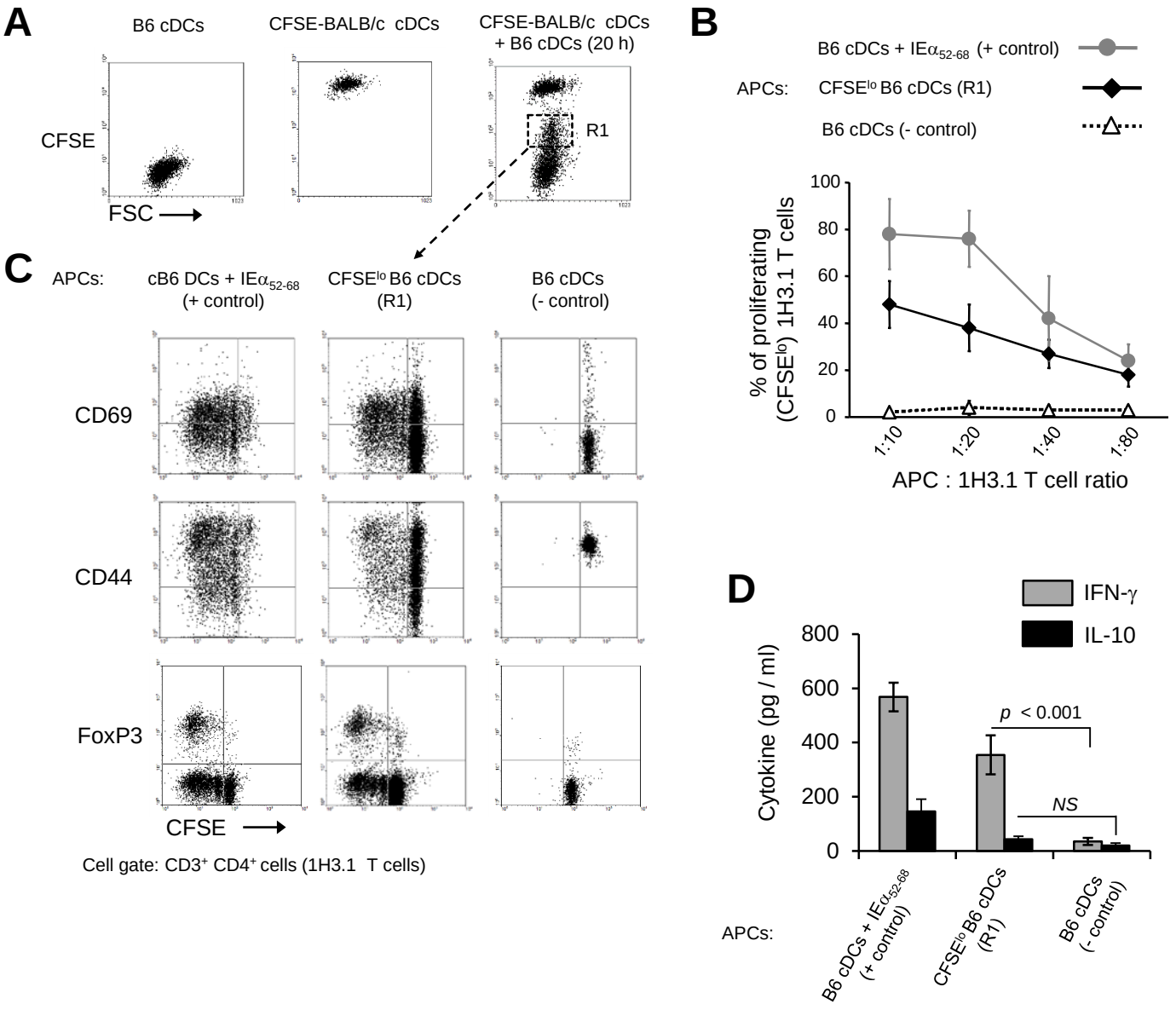

Figure S6. B6 cDCs present allopeptides derived from BALB/c MHC molecules transferred through EVs. (**A-D**) FACS-sorted acceptor B6 splenic cDCs with CFSE^{lo} content (R1 in **A**, carrying the transferred MHC molecules) after 20 hour co-cultures with CFSE^{hi} BALB/c cDCs stimulate proliferation (5 d CFSE-MLCs) (**B**), expression of the T-cell activation markers CD44, CD69 (by FACS) (**C**), and IFN-γ secretion in MLC supernatants (by ELISA) (**D**) in CD4 1H3.1 T cells, the latter specific for the BALB/c-derived IEα_{52-68} allopeptide presented by B6 IA^b molecules. IL-5 and IL-17A in MLC supernatants were undetectable by the ELISAs. *P* values were generated by 1-way ANOVA followed by Tukey-Kramer multiple comparisons test. In (**A-D**) one representative out of 3 independent experiments is shown.

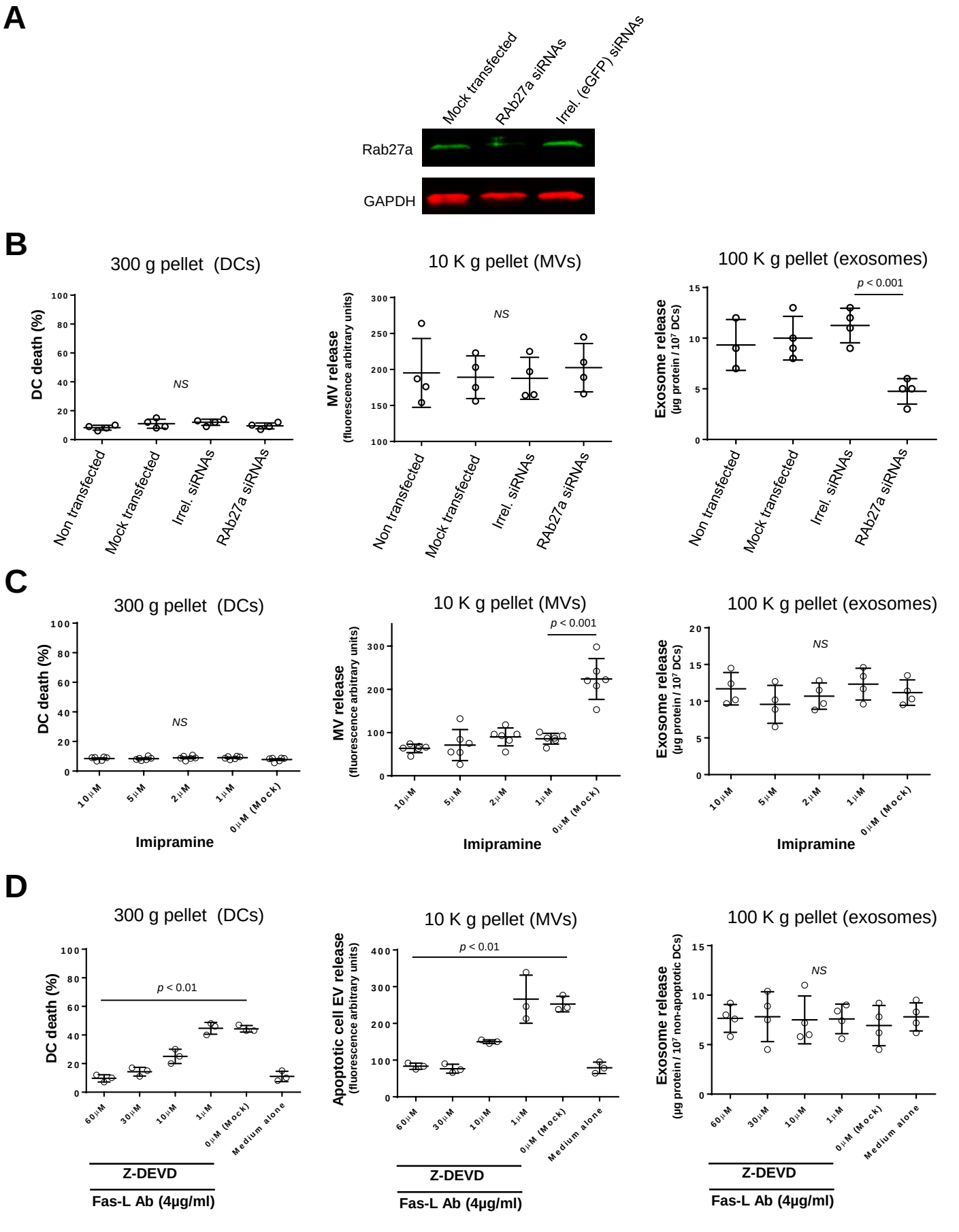

Figure S7 legend (next page).

Figure S7. Quantification of amount of exosomes, MVs and apoptotic cell-derived EVs released by BMDCs under different conditions. (**A**) Analysis by PAGE and Western blot of content of Rab27a protein in mouse BMDCs, 48 hours after transfection with viromers containing mouse Rab27a siRNAs, eGFP siRNAs (irrelevant control), or no siRNA (mock transfected). One representative Western blot out of 2 is shown. (**B**) Cell viability and release of MVs and exosomes to culture supernatants by BMDCs untreated (non transfected), or after transfection with viromers, empty (mock transfected), or carrying eGFP (irrelevant) siRNAs or mouse Rab27a siRNAs. (**C**) Cell viability, and release of MVs and exosomes to culture supernatants by BMDCs left untreated or exposed to increasing concentrations of the drug imipramine. (**D**) Effect of Z-DEVD on cell viability, and release of apoptotic cell-derived EVs and exosomes by BMDCs incubated (16 hours) with the anti-Fas-L Ab Jo2 plus protein G. In (**B-D**), BMDC death was measured by FACS after labelling with PE-annexin-V plus 7AAD. One representative out of 2 experiments is shown. *P* values were generated by 1-way ANOVA, followed by Tukey-Kramer multiple comparisons test. The different types of EVs were isolated as detailed in **Figure S8.**

Culture supernatants from
PKH26-labeled BALB/c BMDCs

↓

300 g (10 min)

↓

10,000 g (30 min)

↓

10 K g pellet

↓

Wash

↓

10,000 g (30 min)

↓

10 K g pellet
(enriched in MVs and apoptotic cell-derived EVs)

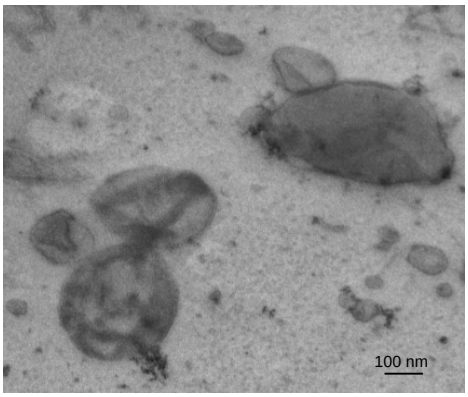

↓

Analysis of PKH26 fluorescence
by spectrophotometry

Culture supernatants from
unlabeled BALB/c BMDCs

↓

300 g (10 min)

↓

10,000 g (30 min)

↓

10 K g supernatant

↓

0.22 µm filtration

↓

30% sucrose / D_2O gradient, 100,000 g (90 min)

↓

Wash

↓

100,000 g (90 min)

↓

100 K g pellet
(enriched in exosomes)

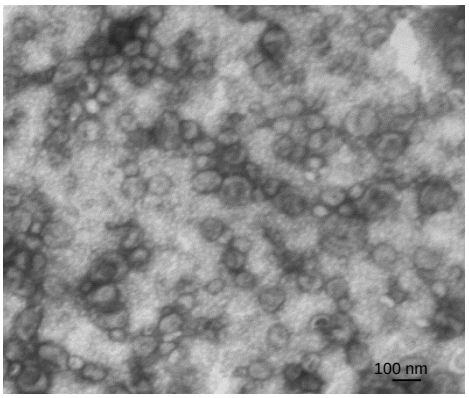

↓

Analysis of protein concentration by spectrometry

Figure S8. Strategy for isolation, based on differential centrifugation, of MVs, apoptotic cell-derived EVs, and exosomes released to culture supernatants by mouse BMDCs under different conditions. EM, X 150,000.

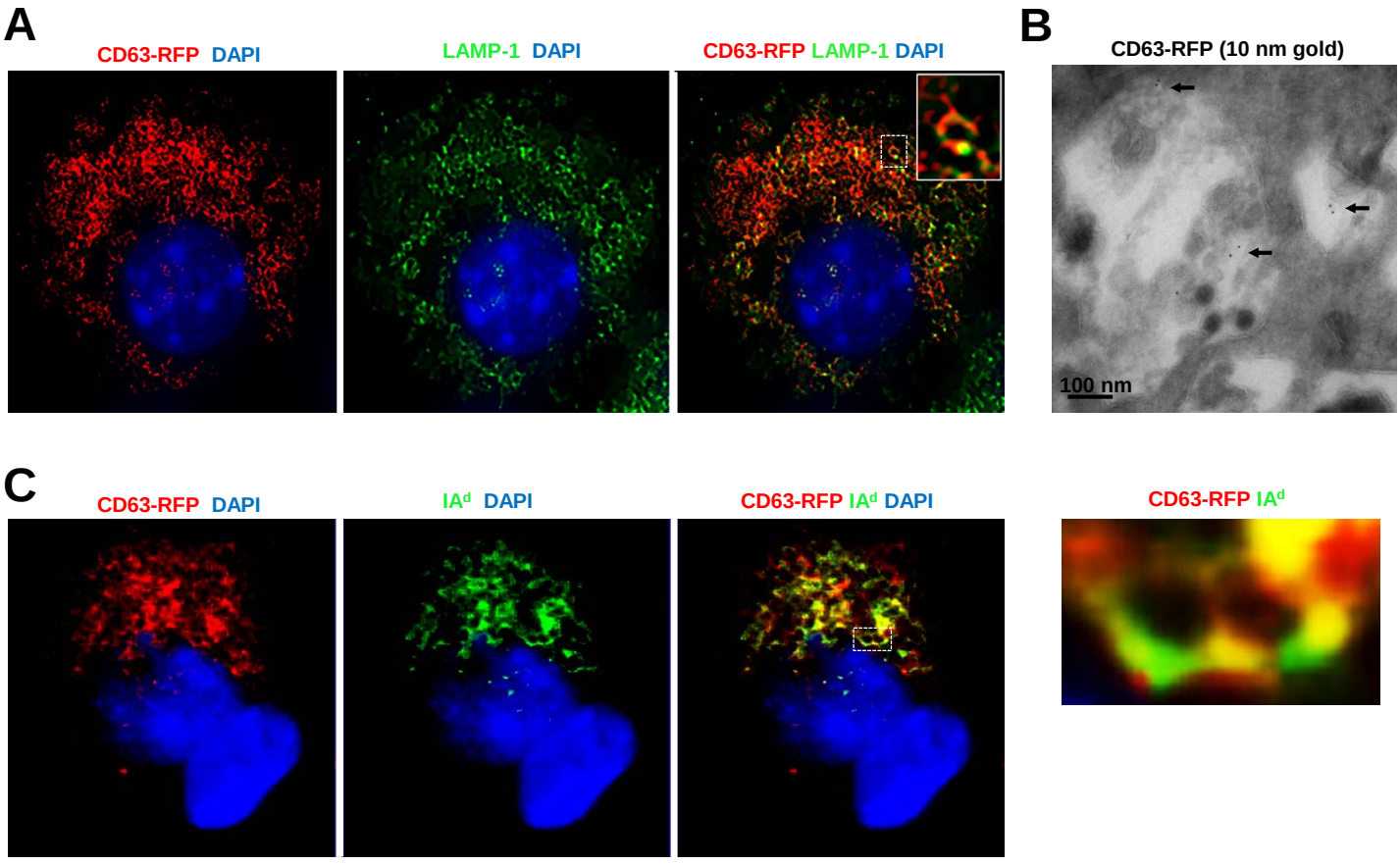

Figure S9. Co-localization of transgenic CD63-RFP and IA^d molecules in MVBs containing exosomes in BMDCs. (**A**) 3-D deconvolution confocal microscopy of a BALB/c BMDC transduced with RAd-CD63-RFP, which shows the association of transgenic CD63-RFP (red) with LAMP-1$^+$ vesicles (green). The area inside the dotted line rectangle is shown at higher magnification. (**B**) Transmission EM image showing the sorting of transgenic CD63-RFP (10 nm gold, arrows, detected with GFP/RFP Ab) into exosomes inside MVBs of a BALB/c BMDC transduced with RAd-CD63-RFP. (**C**) 3-D deconvolution confocal microscopy indicating the localization of transgenic CD63-RFP in relationship to IA^d molecules in a BALB/c BMDC transduced with RAd-CD63-RFP. The area in the dotted line rectangle is shown at higher magnification on the right. In (**A-C**) images are representative cells from 2 independent experiments. Nuclei are stained blue with DAPI. Confocal microscopy , X 400-1000. Transmission EM, X 60,000.

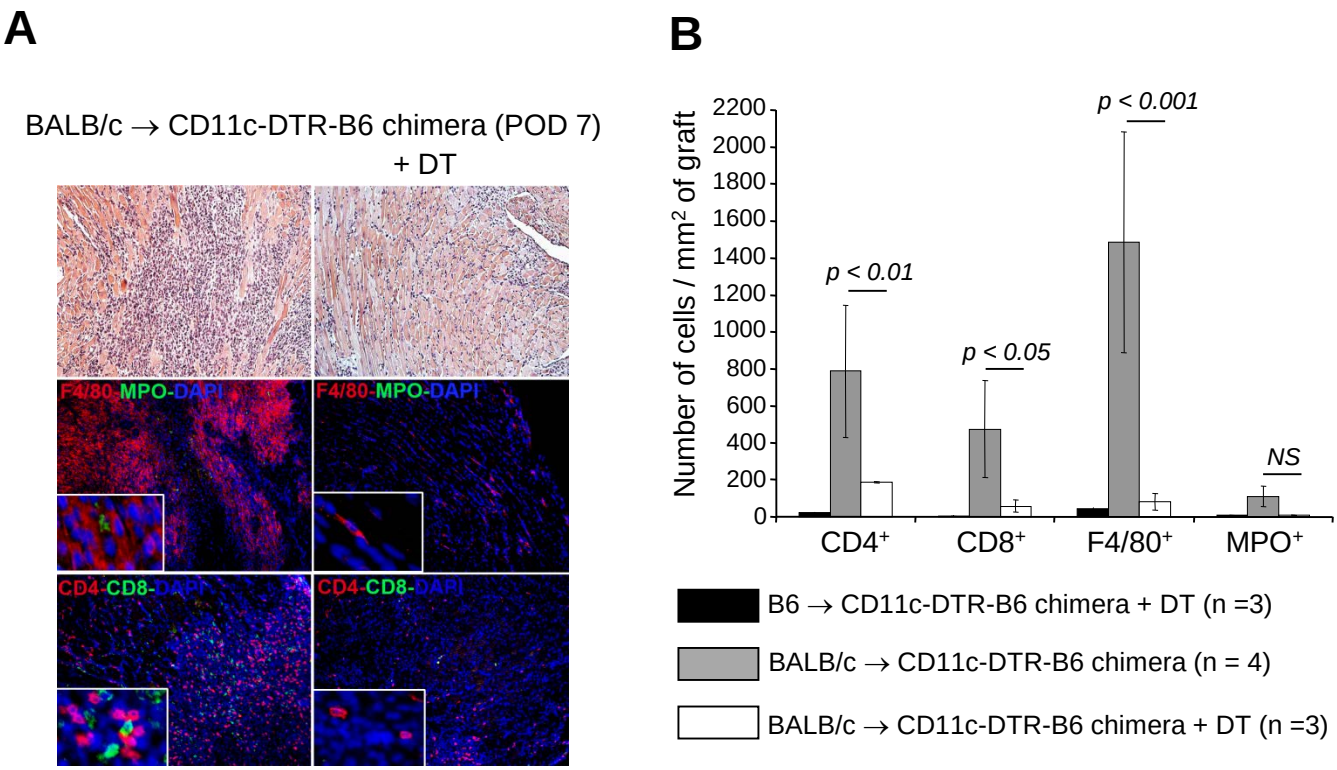

Figure S10. Effect of depletion of recipient cDCs on cardiac allografts. (**A**) Analysis of histology (H&E) and leukocyte infiltrate (by immunofluorescence) of BALB/c cardiac grafts, 7 days after transplantation in CD11c-DTR-B6 chimeras depleted of cDCs (or not, control) by DT-injection. MPO: myeloperoxidase. Images are representative of 3-4 grafts per group. X 200. (**B**) Bar diagram showing average density of graft-infiltrating leukocytes from results pooled from 3-4 grafts per group. Graft-infiltrating cells were counted with the MetaMorph Offline 7.7.50 software. *P* values were generated by 1-way ANOVA followed by Tukey-Kramer multiple comparisons test.

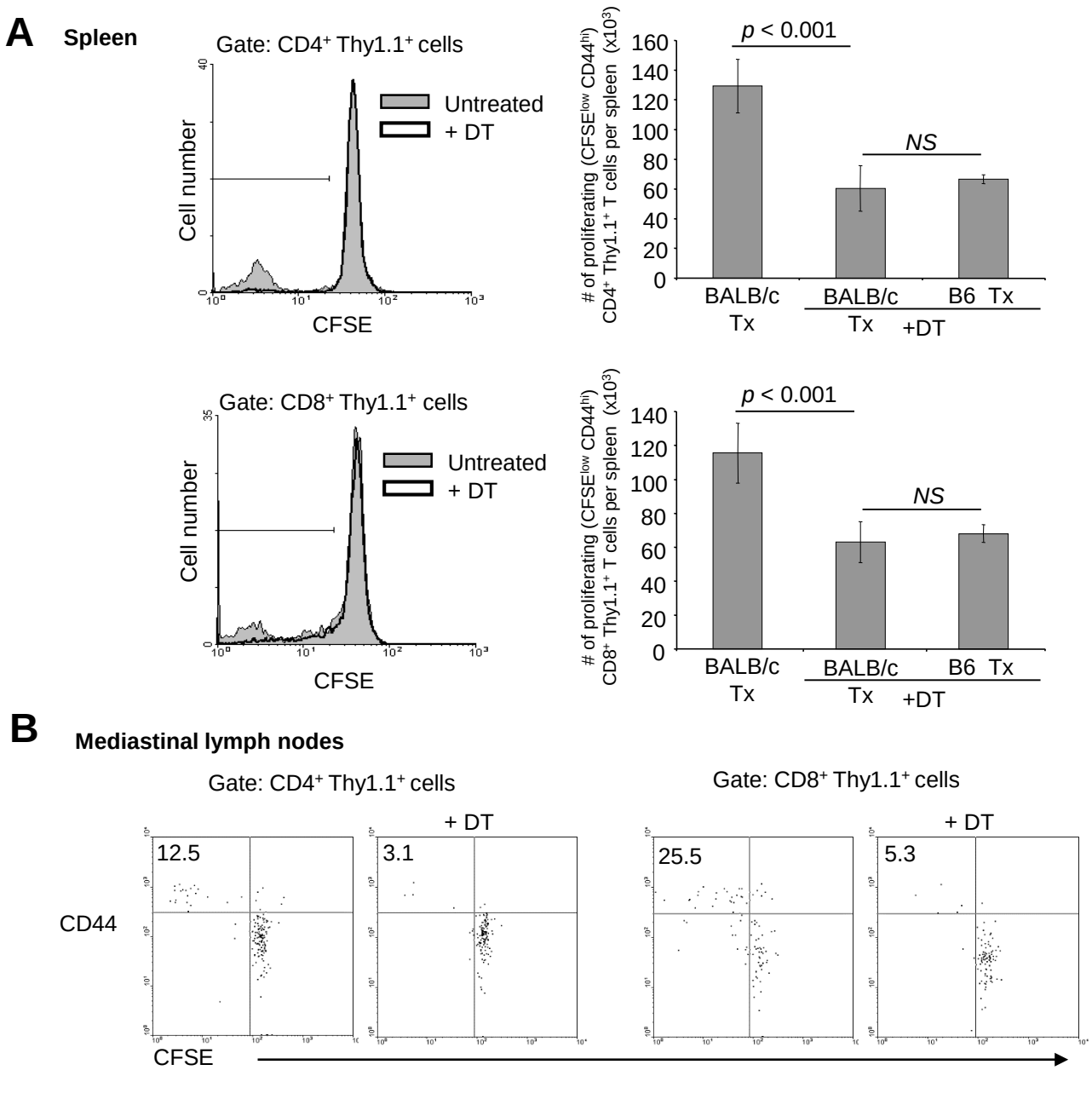

Figure S11. Ablation of recipient cDCs impairs allo-sensitization of adoptively transferred wt T cells after cardiac transplantation. (**A**) DT-injection in CD11c-DTR-B6 chimeras grafted with BALB/c hearts (both Thy1.2), decreased proliferation of i.v. transferred CFSE-labeled Thy1.1 congenic B6 CD4 (top) or CD8 (bottom) T cells (not susceptible to DT) to levels similar as those detected in syngeneic transplants. Bar diagrams: quantification of proliferation of the i.v. transferred T cells. Results are representative of 3 mice per group. *P* values were generated by 1-way ANOVA followed by Tukey-Kramer multiple comparisons test. (**B**) FACS-analysis on POD 7 of mediastinal lymph nodes draining the cardiac allograft showing proliferation (CFSE dilution) and activation (CD44 expression) of Thy1.1 congenic B6 CD4 or CD8 T cells injected i.v. in CD11c-DTR-B6 chimeras, the latter cDC-depleted (or not, control) by repetitive DT-injection, and transplanted with BALB/c hearts. Numbers are percentages of cells in dot plot quadrants. Results are representative of 3 animals per group.

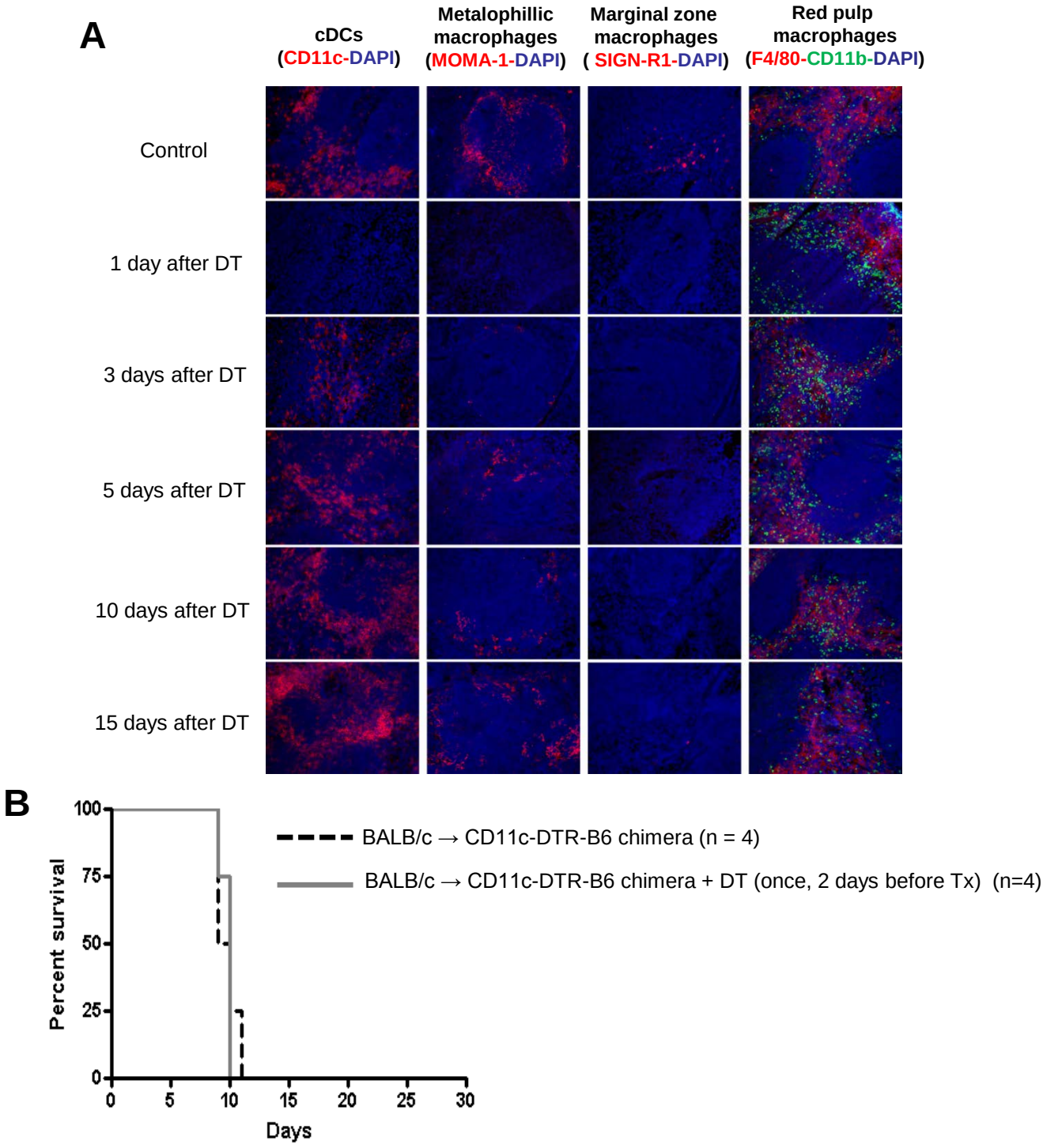

Figure S12. Effect of ablation of splenic macrophages on acute rejection of cardiac allografts. (**A**) Effect of DT-injection on depletion and recovery of cDCs and phagocytes of the marginal zone in spleens of CD11c-DTR-B6 chimeras DT-injected once on days 1, 3, 5, 10 or 15 before analysis. Unlike cDCs, marginal zone phagocytes begin to recover in number 7 days after DT-injection. Images representative of 5-6 sections of 2 mice per time point. AF647-CD11b staining was converted digitally into green. X200. (**B**) Survival of BALB/c hearts in CD11c-DTR-B6 chimeras, left untreated (control) or DT-injected once 2 days prior to transplant (Tx), so the recipient cDCs, unlike the marginal zone phagocytes, are recovered in number at the time of transplant surgery. The splenic marginal zone phagocytes are not required for rejection of the allograft in our model, since both groups reject the allografts with similar kinetics. The numbers of animals per group are in parenthesis.

Supplemental video legends

Video 1: Migrating DCs in lymph nodes transfer exosome clusters to lymph node-resident cDCs. A single Z-stack layer of a 3-D video taken by confocal microscopy of a popliteal lymph node from a CD11c-YFP B6 mouse that was injected (ipsilateral footpad) 16 hours earlier with CD63-RFP BALB/c BMDCs containing RFP-exosomes in its MVBs. The nuclei of the CD63-RFP BALB/c BMDCs were labeled blue with Hoechst. MVBs containing RFP-exosomes are visualized as red dots around the blue nuclei. The lymph node-resident YFP^+ cDCs are in green. The arrow points to a YFP^+ cDC capturing RFP^+ material from a neighboring CD63-RFP BALB/c BMDC.

Videos 2 and 3: Detail of transfer and internalization of clusters of exosomes between migrating BALB/c BMDCs and lymph node-resident B6 cDCs in popliteal lymph nodes. Time-lapse analysis of frontal (video 2) and side (video 3) views of a single Z-stack layer of a 3-D video filmed by confocal microscopy, showing internalization by a lymph node-resident YFP^+ cDC (in green) of RFP-exosome clusters transferred by a CD63-RFP BALB/c BMDC (nucleus in blue).

Video 4: Exosome transfer between migrating BALB/c BMDCs and spleen-resident B6 cDCs. Rotation of a 3-D image taken by multiphoton microscopy of an explant from the spleen of a CD11c-YFP B6 mouse injected i.v. with CD63-RFP BALB/c BMDCs, the latter with nuclei labeled blue with Hoechst and containing/releasing clusters of RFP-exosomes. Numerous splenic YFP^+ cDCs (in green) contain RFP^+ material. The side view section shows the interaction between a CD63-RFP BALB/c BMDCs and an acceptor YFP^+ B6 cDCs.

Video 5: Detail of the passage of exosomes between migrating BALB/c BMDCs and B6 cDCs in the spleen. Time-lapse analysis by confocal microscopy at 3 min intervals of a CD63-

RFP BALB/c BMDCs (nucleus labeled blue with Hoechst) transferring part of its cargo of RFP-exosomes (in red) to neighboring spleen-resident YFP^+ cDCs (in green) of a CD11c-YFP B6 mouse. The image was analyzed with the imaging software Imaris 64X.

Video 6: Some exosome clusters transferred to lymphoid organ-resident cDCs remain on the cDC surface. Time-lapse analysis by confocal microscopy at 3 min intervals of two popliteal lymph node-resident YFP^+ cDCs (in green) with clusters of RFP-exosomes transferred from CD63-RFP BALB/c BMDCs injected in the footpad of CD11c-YFP mice. Most clusters of RFP-exosomes shown remained bound to the surface of the YFP^+ cDC (arrow) during the 4 hour follow up.

Video 7: Fate of exosome clusters transferred between migrating DCs and lymphoid organ-resident cDCs. 360º rotation of a 3-D image showing the fate of RFP-exosome clusters in popliteal lymph nodes of CD11c-YFP mice injected in the footpad with CD63-RFP BALB/c BMDCs, the latter with nuclei labeled blue with Hoechst and containing / releasing RFP-exosomes. Lymph node-resident YFP^+ cDCs are shown in green. The position of the RFP-exosome clusters was determined with the imaging software Imaris 64X. The dots correspond to RFP-exosome clusters, which differ in color according to the position of the RFP-exosomes in relation to the lymph node-resident YFP^+ cDCs. RFP-exosome clusters internalized by YFP^+ cDCs are represented with yellow dots, the ones bound to YFP^+ cDCs with red dots. The light blue dots correspond to RFP-exosome clusters still inside MVBs of CD63-RFP BALB/c BMDCs, free in the extracellular space, or associated to host YFP^- cells.

Video 8: Traffic of control RFP BALB/c BMDCs in popliteal lymph nodes. Time-lapse analysis by confocal microscopy of transfer of cytosolic RFP between RFP^+ BALB/c BMDCs

(injected as a control in the footpad, 16 hours earlier) and lymph node-resident YFP^+ cDCs (in green) of CD11c-YFP mice.

Supplemental methods

Flow cytometric analysis of DCs. Spleens from CD45.1 B6 mice, untreated (control) or transplanted with CD45.2 BALB/c hearts 1, 2, 3 or 7 days before, were removed, teased apart with fine forces, and digested with 400 U/ml type IV collagenase (1 hour, 37^{o}C) pipeting the fragments every 15 min. Next, single cells and tissue fragments were passed through 40 µm cell strainers and the cells centrifuged on top of a 16% Histodenz (Sigma) gradient (1700 r.p.m, 20min, 4°C). cDC-enriched suspension were incubated with anti-CD16/CD32 Ab (to block FcR), and then labeled (30min, 4°C) with the following Ab combinations: (i) FITC-Siglec-H, PE-H2K^{d}, PerCP-Cy5.5-CD11c, PE-Cy7-CD45.1, AF700-CD45.2, APC-IA^{d}, and V500-CD8α Abs; or (ii) FITC-Siglec-H, PE-IA^{b}, PerCP-Cy5.5-CD11c, PE-Cy7-CD11b, AF700-CD45.2, APC-CD45.1, and eF450-CD86 Abs. Leukocytes from spleen, and axillary and inguinal lymph nodes, from CD45.1 B6 mice, untreated (control) or transplanted with CD45.2 BALB/c (or control CD45.2 B6) skin grafts 1, 3 or 7 days before, were incubated with anti-CD16/CD32 Ab (to block FcR), and then labeled (30min, 4°C) with the following Ab combinations: PE-H2D^{d}, PE-H2K^{d}, APC-IA^{d}, PerCP-Cy5.5-CD11c, PE-Cy7-CD45.2, eF-450-CD45.1, and v500-C8α Abs. Dead cells were excluded by labeling with the Fixable Viability Dye (eBioscience), and doublets comprising recipient and donor cells were excluded by analyzing exclusively CD45.2^{neg} cells. Appropriate irrelevant Abs were used as controls. Cells were fixed in paraformaldehyde and analyzed with a BD™ LSR II flow cytometer.

***Transmission electron microscopy*.** For in vivo experiments, cDC-enriched suspensions from spleens of B6 mice, transplanted 3 days before with BALB/c hearts, were labeled with PE-H2K^{d}, PerCP-Cy5.5-CD11c, PE-Cy7-CD45.1, and APC-CD45.2 Abs. Recipient splenic cDCs (CD11c^{hi} CD45.1^{+} CD45.2^{-}) carrying donor Ag (H2K^{d+}) were FACS-sorted, kept on ice-cold medium, and re-labeled with biotin-IA^{d} and biotin-H2D^{d} Abs alone, or plus either rat anti-mouse

CD9 Ab or rabbit anti-mouse CD63, followed by 5nm gold-streptavidin, 12nm gold anti-rat Ab or anti-rabbit Ab. Controls were incubated with irrelevant Abs, followed by 5nm gold-streptavidin and 12nm gold anti-rat or anti-rabbit Ab.

For in vitro experiments, splenic cDCs harvested from 20 hour cocultures of unlabeled B6 cDCs with CFSE-labeled BALB/c cDCs (at 1:1 cell ratio), were harvested, labeled with APC-IA^d Ab, and FACS-sorted into $CFSE^{high}$ $IA^{d\ high}$ BALB/c cDCs and $CFSE^{int}$ $IA^{d\ int}$ B6 cDCs. Sorted cells were kept on ice-cold medium and re-labeled with biotin-IA^d and biotin-$H2D^d$ Abs alone, or with CD9, CD63, or CD86 Ab, followed by 5nm gold-streptavidin and 12nm gold-conjugated secondary Abs. Controls were labeled with irrelevant Abs plus 5nm gold-streptavidin and 12nm gold-conjugated secondary Abs. In some experiments, after immunogold labeling, cDCs were rinsed in ice-cold PBS, and incubated in complete medium, in a water bath at 37°C for 30 min, to promote endocytosis of gold-labeled EVs attached to the cell surface.

cDCs labelled with gold pre-embedding were rinsed with ice-cold PBS, pelleted by centrifugation, and the pellets were fixed in cold 2.5% glutaraldehyde in 0.1 M PBS. Alter fixation, the pellets were rinsed in PBS, post-fixed in 1% osmium tetroxide with 0.1% potassium ferricyanide for 30 min, rinsed in PBS, dehydrated through a graded series of ethanol, and embedded in epon. Semi-thin (300 nm) sections were cut on a Reichart Ultracut, stained with 0.5% toluidine blue and examined under the light microscope. Ultrathin sections (65 nm) were stained with uranyl acetate and Reynold's lead citrate and examined on Jeol 1011 transmission electron microscope. The diameters of EVs attached to DCs were measured on transmission EM images with the MetaMorph Offline 7.7.50 software.

Cryosections of pellets of cDC cocultures were labelled post embedding biotin-IA^d and biotin-$H2D^d$ Abs plus 5nm gold-streptavidin. Cryosections of pellets of CD63-RFP BALB/c BMDCs were labelled post-embedding with biotin-RFP Ab followed by streptavidin-10 nm gold.

Assays of Ag-presentation in mixed leukocyte cultures (MLCs). For ex vivo detection of presentation of BALB/c MHC class-I molecules by recipient (B6) splenic cDCs, spleens of CD45.1 B6 mice, transplanted 3 days before with CD45.2 BALB/c hearts, were digested with collagenase, and centrifuged on top of 16% Histodenz gradients. DC-enriched suspensions were labeled with PE-H2K^{d}, PerCP-Cy5.5-CD11c, PE-Cy7-CD45.1, and APC-CD45.2 Abs. Recipient splenic cDCs (CD11c^{hi} CD45.1^{+} CD45.2^{-}) carrying donor Ag (H2K^{d+}) were FACS-sorted and used as stimulators of CFSE-labeled (7.5. µM) 2 CD8 T cells (specific for BALB/c H2L^{d}), in round bottom 96 well plates (1.5x10^{5} T cells / well). After 3 days, cells were labeled with APC-Cy7-CD3, APC-CD8, and BV605-CD44 Abs, in combination with PE-CD107a Ab, or PE-granzyme B Ab (intracellular), and analyzed by FACS.

For detection of presentation of BALB/c MHC class-I molecules transferred to B6 splenic cDCs in vitro, acceptor B6 cDCs with CFSE^{lo} content, donor CFSE^{hi} BALB/c cDCs, and 4µm latex beads (Interfacial Dynamics Corporation, IDC), were FACS-sorted from 20 hour cocultures of CFSE^{hi} BALB/c cDCs with either unlabeled B6 cDCs or latex beads. The sorted cDCs (or control beads) were used as stimulators of CFSE-labeled 2C T cells in MLCs. After 3 days, proliferation and phenotype of 2C T cells were analyzed by FACS, as aforementioned.

For assessment of presentation of BALB/c-derived allopeptides by B6 splenic cDCs, acceptor B6 cDCs with CFSE^{lo} content were FACS-sorted from 20 hour cocultures of CFSE^{hi} BALB/c cDCs with unlabeled B6 DCs, and used as stimulator of 1H3.1 CD4 T (specific for the BALB/c IE$\alpha_{52\text{-}68}$ peptide loaded in B6 IA^{b}), in round bottom 96 well plates (1.5x10^{5} T cells / well). After 5 days, cells were collected, labelled with APC-Cy7-CD3, PerCP-Cy5.5-CD4, and BV605-CD44 Abs, in combination with PE-CD69 Ab or PE-FoxP3 Ab (intracellular), and analyzed by FACS.

Concentrations of IFN-γ, IL-5, IL-10, and IL-17A were analyzed in MLC supernatants by ELISA according to the manufacturer's protocols (R&D Systems, eBioscience).

***siRNA transfection of BMDCs*.** BMDCs were generated in medium with 10% FCS, GM-CSF (1000 U/ml), and IL-4 (500 U/ml). On day 5, BMDCs were purified with CD11c magnetic beads, γ-irradiated (2000 rads, to block cell division), and placed in ultra-low attachment surface 6 well plates (Corning), at $1.2x10^6$ cells / well, in medium with 10% exosome-free FCS plus GM-CSF (1000U/ml). Cells were then transfected with the Viromer® Blue transfection reagent (Lipocalix) containing 100nM of Mission® endoribonuclease-prepared siRNAs (esiRNAs, Sigma) targeting mouse Rab27a, according to the manufacturer's manual. Controls were transfected with esiRNAs targeting enhanced green fluorescent protein (eGFP), or with Viromer® Blue alone. After 48 hours, cells were harvested for analysis or experimentation.

***In vitro assays of EV release*.** MVs shed from the plasma membrane of BMDCs under different conditions were measured semi-quantitatively in culture supernatants. BMDCs (day 6), purified with CD11c magnetic beads, non-transfected or siRNA-transfected, were labeled red on the cell membrane with PKH26 (Sigma), and incubated in 96 well plates ($2x10^5$ DCs / well) in 200 µl of sucrose solution (300 mM sucrose, 1 mM K_2HPO_4, 1 mM $MgSO_4$, 5.5 mM glucose, 20 mM Hepes, and 1mM $CaCl_2$, pH 7.4) to preserve the MV structure, and with 2',3'-(4-benzoyl-benzoyl)-ATP (200 µM, Sigma) to stimulate MV release. Imipramine hydrochloride (1-10 µM, Sigma) was added as inhibitor of MV shedding. After 60 min (37ºC, 5% CO_2), supernatants were centrifuged at 300 g (10 min), and 10,000 g (30 min). Pellets containing the MVs were rinsed, resuspended in 100 µl of sucrose solution, and the PKH26 fluorescence was assayed at 470/502 nm by spectrophoto-metry (Synergy 4, Biotek).

Apoptotic cell-derived EVs released by BMDCs to culture supernatants were measured semi-quantitatively with a similar methodology. BMDCs (day 6) purified with CD11c magnetic beads were labeled on the cell membrane with PKH26, and placed in 24 well plates ($5x10^5$ BMDCs / well) in medium with 10% exosome-free FCS, the anti-Fas-L Ab Jo2 (4 µg / ml), and protein G (2 µg / ml, Sigma). Z-DEVD (1-60 µM, MBL) was added as apoptosis inhibitor. After

16 hours (37ºC, 5% CO_2), supernatants were centrifuged at 300 g (10 min), and 10,000 g (30 min). Pellets containing the apoptotic cell-derived EVs were rinsed, resuspended in 100 µl of PBS, and the PKH26 fluorescence was assayed by spectrophotometry, as aforementioned.

To measure the amount of exosomes released by BMDCs under different conditions, the respective culture supernatants from BMDCs (not labeled with PKH26) were centrifuged at 300 g (10 min) and 10,000 g (30 min), and then passed through a 0.22 µm filter. The filtered supernatants were centrifuged at 100,000 g (90 min) on top of 30% sucrose/D_2O. The phase containing the exosomes was collected, rinsed in PBS, and centrifuged at 100,000 g (90 min). The pellets were resuspended in 100 µl pf PBS, and the amount of exosome protein was measured by spectrometry with a NanoDrop 2000c.

***SDS-PAGE and Western Blot analysis*.** EVs and siRNA-transfected BMDCs were resuspended in RIPA buffer (Sigma). Next, samples were diluted in 4x LDS sample buffer with or without 10x sample reducing agent (Invitrogen), incubated on a heating block (95ºC, 5 min), and loaded in 4%-20% gradient acrylamide pre-cast gels (BIO-RAD). Gels were electroblotted on polyvinylidene difluoride membranes (BIO-RAD). For EV analysis, membranes were labeled with Abs against GP96, CD81, HSP70 and CD86. For analysis of siRNA-transfected BMDCs, membranes were probed with Abs against Rab27a and GAPDH. Next, membranes were incubated with the appropriate secondary Abs conjugated with IRDye 680 or 800 (Li-Cor). Staining was measured with an Odyssey Infrared Imager (Li-Cor).

***Immuno-fluorescence microscopy*.** For analysis of traffic of donor DCs after heart (abdomen) transplantation, cryostat sections of spleens and retroperitoneal and mediastinal lymph nodes were fixed, treated with 5% normal goat serum followed by the avidin/biotin blocking kit (Vector). Spleen sections were incubated with biotin-IA^b, AF488-IA^d, and rat anti-mouse CD3 Abs, followed by Cy3-streptavidin plus Cy5-anti rat IgG; or with biotin-YAe, AF488-IA^d, and

hamster anti-mouse CD11c Abs, followed by streptavidin-Cy3 and Cy5-anti hamster IgG. Lymph node sections were incubated with: (i) AF-488-IA^d Ab, biotin-IA^b Ab followed by Cy3-streptavidin, and rat anti-mouse CD3 Ab plus AF-647-conjugated anti-rat IgG; or (ii) AF-488-IA^d Ab, biotin-CD45.2 Ab followed by Cy3-streptavidin, and hamster anti-mouse CD11c Ab plus Cy5-conjugated anti-hamster IgG. Nuclei were stained with DAPI.

Paraffin-embedded heart allograft sections were processed for H&E. Graft fragments were snap-frozen in liquid N and stored at -80°C until use. Cryostat sections (10 μm) were fixed in 95% ethanol, and blocked as aforementioned. Tissue sections were stained with (i) biotin-CD4 and AF488-CD8 Abs, followed by Cy3-streptavidin; or (ii) purified anti-myeloperoxidase (MPO) rabbit serum and biotin-F4/80 Ab, followed by Cy2-anti-rabbit IgG and Cy3-streptavidin. Nuclei were stained with DAPI. Slides were examined with a Nikon Eclipse E800 microscope equipped with a CCD camera. Leukocyte infiltrates were quantified at 200 X, on 5 sections per allograft, with the MetaMorph Offline 7.7.50 software.

For assessment of depletion and recovery of cDCs and macrophages in CD11c-DTR-B6 BM chimeras, cryostat sections of spleens of animals DT-injected at different days before euthanasia, were fixed with ethanol, and blocked as mentioned above. Sections were incubated with biotin-CD11c, biotin-MOMA-1, biotin-SIGN-R1, biotin-F4/80, or AF647-CD11b Abs, followed by Cy3-streptavidin. Nuclei were stained with DAPI.

CD63-RFP BALB/c BMDCs were seeded on poly L lysine pre-treated slides (1 hour, 10 ºC), fixed in 4% paraformaldehyde, permeabilized in PBS / 0.1% BSA / 0.05% saponin , and incubated with LAMP-1 or IA^d Ab (or the species and isotype Ig controls), followed by AF488-conjugated secondary Ab. Nuclei were stained with DAPI.

***ELISPOT assays*.** For analysis of the direct pathway response, purified splenic T cells (enrichment columns, R&D Systems) from naïve B6 control mice, or from CD11c-DTR-B6 BM chimeras transplanted with BALB/c hearts were incubated with CD3-depleted, γ-irradiated,

splenic B6, BALB/c or C3H APCs ($3x10^4$ T cells + $2.5x10^5$ APCs / well) in 96-well ELISPOT plates coated with IFN-γ Ab.

To quantify the indirect pathway response, purified recipient splenic T cells were incubated with CD3-depleted, γ-irradiated, splenic B6 APCs ($3x10^5$ T cells + $2.5x10^5$ APCs / well) and sonicates (50μl/well) prepared from BALB/c, B6 or C3H splenocytes (from $2x10^7$ cells / ml). All cultures were done in serum-free HL-1 medium. ELISPOT plates were developed 36 hours later (BD Biosciences).

***Detection of anti-donor Abs*.** The titer of anti-donor Abs in serum was determined by FACS-analysis. Target (BALB/c) and control (B6) splenocytes were incubated for 30 min at 4°C with serial dilutions of serum from naïve B6 mouse controls or from CD11c-DTR-B6 BM chimeras transplanted with BALB/c hearts. Next, cells were rinsed and incubated with FITC-$F(ab')_2$ fragment goat anti-mouse IgG Fcγ fragment, and analyzed by flow cytometry.

***Analysis of adoptively transferred T cells in graft recipients*.** CFSE-labeled Thy1.1 B6 splenic naïve T cells were adoptively transferred (i.v., 50 x 10^6 cells) in CD11c-DTR-B6 BM chimeras (Thy1.2), 1 day before transplantation of BALB/c or B6 (control) hearts. Recipients were depleted (or not, control) of recipient cDCs by injection of DT (i.p., 4ng/ g body weight), starting 1 day before transplant surgery and every 48 hours. On POD7, recipient spleen and mediastinal lymph nodes were harvested, teased apart and passed through 40 µm cell strainers, and erythrocytes were depleted with NH_4Cl solution. Spleens and mediastinal lymph nodes cells were labelled with PE-CD4, APC-Cy7-CD8, PerCP-Cy5.5-CD44, and APC-Thy1.1 Abs, and analyzed by FACS.

Amnis ImageStream® analysis. cDC-enriched suspensions were generated by 16% Histodenz gradient centrifugation of splenic leukocytes isolated from CD45.1 B6 mice, transplanted 3 days before with CD45.2 BALB/c skin grafts. cDC-enriched suspensions were labeled with AF488-IA^d, PE-$H2K^d$, PE-$H2D^d$, PerCP-Cy5-CD11c, APC-CD45.1, and APC-Cy7-CD63 Abs. Cell nuclei were stained with DAPI, and cells were fixed in 4% paraformaldehyde. Five thousand cells were collected with a two-laser Amnis ImageStream® analyzer, at a magnification X 60. Cell images were analyzed with the software IDEAS v6.2.